Environ Health Eng Manag 2026;13:1508
http://ehemj.com
doi:10.34172/EHEM.1508

Environmental Health Engineering and Management Journal

Original Article

Open Access Publish Free

Adsorption Studies of Cd(II) and Zn(II) onto Polypyrrole/ Sb_2O_3 Nanocomposite: Kinetics, Equilibrium, and Thermodynamics

Zeynab Karimi[1], Soheil Balsini Gavanaroudi[2], Saeid Sabzehali[3], Amirhossein Alidadi[4], Ali Akbar Amooey[5], Reza Khalili[6*]

[1]Department of Environmental Health Engineering, Faculty of Health, Student Research Committee, Mazandaran University of Medical Science, Sari, Iran
[2]Department of Chemical Engineering, Youngstown State University, Ohio, United States of America
[3]Isfahan University of Technology, Graduate with an M.sc in Materials Science and Engineering, Isfahan, Iran
[4]Bachelor of Mechanical Engineering, Faculty of Technical Engineering, Azad University, North Tehran Branch, Tehran, Iran
[5]Department of Chemical Engineering, University of Mazandaran, Babolsar, Iran
[6]Faculty of Engineering and Technology, University of Mazandaran, Babolsar, Iran

Abstract

Introduction: Heavy metal ions are very toxic to public and personal health. A special polypyrrole with environmental stability and reusability was used to remove metal ions from aqueous solution. In this work, a new polypyrrole (PPy/Sb_2O_3) nanosorbent was successfully synthesized in aqueous solution.

Methods: The purpose of this research was to investigate the adsorption properties of polypyrrole nanocomposites for the removal of Cd(II) and Zn(II) from aqueous solution. Batch various factors affecting the adsorption equilibrium were investigated in detail. Also, different models (isotherm, kinetic, and thermodynamic) were compared to describe the adsorption phenomenon.

Results: The adsorption isotherms for Cd(II) and Zn(II) were well fitted by the Langmuir model with a maximum monolayer capacity of 17.33 and 15.361 mg/g, respectively, for Cd (II) and Zn (II) ions. Moreover, thermodynamic analysis shows the endothermic nature and spontaneity of the adsorption process with increasing entropy in PPy-PVA/Sb_2O_3. From the kinetic results, it was concluded that the pseudo-second-order kinetic model is the best in describing the adsorption process for Cd (II) and Zn (II). The consistency of the experimental qe with the qe calculated from the pseudo-second-order kinetic model indicated that the adsorption of Cd(II) and Zn(II) on PPy-PVA/Sb_2O_3 is probably controlled by chemisorption.

Conclusion: This study shows that polypyrrole and its nanocomposites have a potential for use as effective adsorbents due to their ease of synthesis, low cost, and regeneration efficiency for the removal of heavy metal ions from aqueous solutions.

Keywords: Polypyrrole, Adsorption, Nanocomposite, Isotherm, Thermodynamic

Citation: Karimi Z, Balsini Gavanaroudi S, Sabzehali S, Alidadi A, Amooey AA, Khalili R. Adsorption studies of Cd(II) and Zn(II) onto polypyrrole/Sb_2O_3 nanocomposite: Kinetics, equilibrium, and thermodynamics. Environ Health Eng Manag 2026;13:1508. doi:10.34172/EHEM.1508

Article History:
Received: December 31, 2024
Revised: July 27, 2025
Accepted: August 5, 2025
ePublished: August 29, 2026

***Correspondence to:**
Reza Khalili,
Email: khalili504@yahoo.com

Introduction

Water pollution by various pollutants such as heavy metal ions, paints, oils, pharmaceuticals, and nutrients is one of the most important environmental and health problems. Heavy metal ions such as iron, lead, chromium, cobalt, zinc, arsenic, copper, nickel, mercury, and cadmium are among the persistent pollutants in wastewater (1-3). The release of heavy metals in the environment, which is mainly caused by human activities, even at low concentrations due to high solubility in water and soil, high toxicity, and non-biodegradable nature, causes dangerous effects on plants, animals, and living organisms (4,5). It also causes bioaccumulation and biomagnification in the food chain. Heavy metals such as Cd(II) and Zn(II) exposure causes serious health effects, including cancer, organ damage, nervous system damage, lung damage, damage to the brain, and eventually leads to death. Therefore, the heavy metal ions in wastewater should be removed before the water is discharged into the environment.

To remove heavy metals from the contaminated wastewater, various treatment approaches such as ion-exchange (6), coagulation–flocculation (7), physical and chemical precipitation (8), membrane filtration (9), electrochemical treatment (10), reverse osmosis (11) and adsorption processes (12) have been employed. Most of these methods are effective but require large amounts of chemicals and high energy. Among the approaches, absorption technology is the best method in wastewater treatment due to its significant advantages, including cheap materials, availability, ease of use, and high efficiency compared to other conventional methods (13-15). To achieve high absorption efficiency in wastewater, special attention should be paid to the design and synthesis of adsorbents with high absorption capacity (16-18). Recent studies have focused on many interesting adsorbents such as fly ash (19), graphene oxide and reduced graphene oxide (20), inorganic minerals (21), active carbon (22), zeolites (23), and biosorbents (24). However, most of these adsorbents have weaknesses such as low adsorption capacity and slow kinetics, difficulty separating after purification, and low surface area. Therefore, finding new adsorbents with high adsorption performance is still challenging (25). Recently, conducting polymers such as polyaniline (PANi), polypyrrole (PPy), and polythiophene (PTh) with interesting stability and doping capabilities have been introduced as adsorbents for the adsorption of heavy metal ions from aqueous solutions (26,27). Their availability, easy preparation, and performance make them desirable in many applications. Among conductive polymers, polypyrrole (PPy) is one of the most frequently studied polymers, which has many advantages including non-toxicity, good biocompatibility, easy synthesis, high environmental stability, low cost, and ion exchange properties (28). In polymer chains, PPy has positively charged nitrogen atoms that may easily bind heavy metal ions (29). There are various methods for the synthesis of conducting polymers, among which the in-situ polymerization method is of particular importance. The advantages of this method include the ability to produce polymer products with the required properties and characteristics by adjusting the process conditions, ease of carrying out the process, reducing waste and production costs, and reducing production time (30).

Therefore, in the present study, it has been tried to use chemically modified polypyrrole with antimony oxide (PPy/Sb_2O_3) in the presence of poly(vinyl alcohol) to remove Cd(II) and Zn(II) ions from water. The batch equilibrium method was used to study the adsorption process. PPy/Sb_2O_3 composites were analyzed by FTIR, XRD, and SEM. Factors affecting the absorption process, such as pH, time, and temperature, were investigated. Also, based on the experimental results, adsorption kinetics, equilibrium, and thermodynamics were discussed.

Materials and Methods

Instrumentation

A digital scale model D-500, pH meter model HANA211, centrifuge model Z36HK, Fourier transform infrared (FTIR) spectrometer (Avatar 370, Nicolet, USA) within the 400-4000 cm^{-1} range, X-ray diffraction (XRD) with Cu Kα radiation (X'Pert Pro, Panalytical, Netherlands), flame atomic absorption spectrophotometer model Thermo electrene, scanning electron microscope (SEM) model KYKYEM3200, oven Binder model FD 23 and magnetic mixer model MK20 (Germany) were employed.

Materials

Materials used in this study were monomer of pyrrole (d = 0.97 g/cm^3) from Aldrich, poly(vinyl alcohol) (PVA), ferric chloride, and antimony oxide (Sb_2O_3), which were obtained from Merck (Germany). All reagents were used as received. During this research, deionized water was used, and pyrrole monomers were purified using distillation.

Synthesis of polypyrrole/Sb2O3 in the presence of PVA

An in situ chemical polymerization method was used to prepare the nanosorbent. For the synthesis, 5 g of $FeCl_3$ was added to 50 mL distilled water. 0.2 g of PVA and 1.0 g of Sb_2O_3 were dissolved in 50 mL distilled water; a uniform solution was achieved using a magnetic mixer for 30 min and added to the oxidant solution. Finally, 1 mL of pyrrole monomer was added to a stirred aqueous solution, which was maintained under constant stirring. The reaction was carried out for 5 h at room temperature. The product was collected by filtration. To separate the oligomers and impurities, the product was washed several times with deionized water. It was then dried at about 60°C in an oven for 24 h. A pure PPy was synthesized using the same method used previously, without Sb_2O_3 and PVA (100 mL distilled water containing 5 g $FeCl_3$ and 1 mL pyrrole monomer).

Batch adsorption experiment

Adsorption experiments in this study were conducted to investigate the effects of experimental conditions on the adsorption of Cd(II) and Zn(II) and to determine the conditions that obtain the maximum removal of metal ions. The standard heavy metal solutions used in the study were prepared from $CdCl_2$ and $Zn(NO_3)_2$, respectively, with deionized water. The pH values of the solution in these experiments were approximately 2-7. To determine the amount of removal of metal ions by nanocomposites, the solution of metal ions (50 mg/L) was mixed with 0.3 g of powder adsorbent. 30 mL of heavy metal solution was placed in a shaker at a speed of 400 rpm for 45 minutes to carry out the adsorption process. At the end of the process, the adsorbent was filtered. The amount of metal ions in the solution after the adsorption process was measured by atomic absorption. All experiments were performed twice to obtain average values. The deviation of this method was less than 5%. The pH of the solution was adjusted using 0.1 mol/L NaOH and 0.1 mol/L HNO_3, and the pH was measured with a digital pH meter.

The removal efficiency of Cd(II) and Zn(II) and the amount of metal ions adsorbed per specific amount of adsorbent at equilibrium (mg/g), q_e were calculated as:

$$\text{Removal efficiency } (\%) = 100 * {(C0-Ce)}/{C0} \quad (1)$$

$$qe = {(C0 - Ce)V}/{m} \quad (2)$$

Where q_e is the amount of metal adsorbed per specific amount of adsorbent (mg/g), C_0 and C_e are the initial and equilibrium solution concentrations (mg/L), respectively, V is the volume of solution (L), and m (g) is the weight of adsorbent.

Results

Characterization of nanocomposites

Figure 1 depicts the FTIR spectra of (a) PPy, (b) PPy-PVA, (c) PPy/Sb_2O_3, and (d) PPy-PVA/Sb_2O_3. The peaks seen at 1541, 1299, 1166, 1044, 895, and 789 cm^{-1} are matched to stretching vibrations of the C = C, C–N, C–H in-plane deformation, C–H out-of-plane ring deformation, and N–H in-plane deformation, and C–H out-of-plane deformation (31). According to Figure 1, the intensity or wavenumber of the peaks of PPy varies slightly in the samples that were modified with PVA and Sb_2O_3. The reason for this event is the interaction between polypyrrole, surfactant, and additive and changes in bonding energies.

The crystalline nature of the composites appeared from XRD analysis. Figure 2 shows the XRD patterns of (a) PPy, (b) Sb_2O_3, and (c) PPy/Sb_2O_3. For pure polypyrrole, the main diffraction peaks were observed at $2\theta = 26.41°$ and for Sb_2O_3, diffraction peaks were observed at $2\theta = 19.07°$, $2\theta = 26.33°$, $2\theta = 29.41°$, and $2\theta = 49.83°$. The XRD pattern of PPy/Sb_2O_3 reveals distinct crystalline peaks corresponding to the antimony oxide and polypyrrole, and this feature further supported the successful grafting of PPy onto the Sb_2O_3. The crystallinity of the composite is caused by the crystalline structure of Sb_2O_3.

Morphological characterization of composites was investigated using a scanning electron microscope. The SEM of polypyrrole composites is shown in Figure 3. Polypyrrole composites have a porous and spherical structure in aqueous media (32). Figure 3b shows the PPy-PVA nanocomposite. It is apparent from Figures 3a and 3b that the surface morphology of polypyrrole has been considerably changed after the introduction of PVA into the polymeric matrix. Using surfactant decreases the tendency to form accumulations, because surfactant is prevented from aggregation of the particles, and the surface of PVA is covered with dispersed PPy Particles (33). As can be seen in images 3c and 3d, by adding Sb_2O_3, the size of the particles decreased and the uniformity of the particles increased. The reaction mixture is dispersed in particles, and therefore, all the Sb_2O_3 around the particles is covered with the polymer.

Effect of pH

According to the SEM micrographs of the composites, among the synthesized composites, PPy-PVA/Sb_2O_3 had the most uniform shape and special characteristics. Therefore, the removal experiments were performed using this adsorbent. One of the influential parameters in the adsorption process is the pH of the solution to control the amount of metal ions on the surface of the adsorbent.

The removal efficiency was investigated at different pH values ranging from 2 to 7 while other factors such as the concentration of metal ions, contact time, and temperature remained constant. At pH values higher than 7, removal experiments were not performed due to the formation of cadmium hydroxide and zinc hydroxide, which leads to a misinterpretation of the adsorption process.

Figure 4 shows the effect of solution pH on the removal of Cd(II) and Zn(II) ions using PPy-PVA/Sb_2O_3. The removal of Cd(II) and Zn(II) ions increased with increasing pH, and the maximum removal percentage of Cd(II) and Zn(II) ions occurred at pH 5 and 6, respectively. At lower pH values, protonation of the adsorbent surface may be possible (34). In addition, due to the high concentration of H^+ ions, it may compete with the ions present in the active sites of the adsorbent, which reduces the adsorption of metal ions. When the pH increases, the competition between H^+ ions and Cd^{2+} and Zn^{2+} ions in the active sites of the adsorbent decreases, which leads to the improvement of the adsorption process.

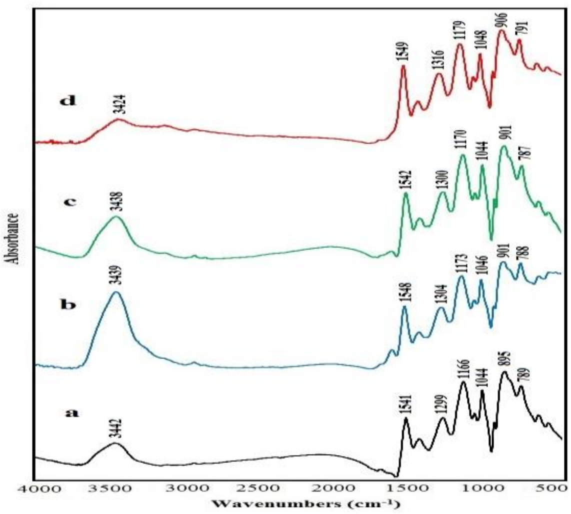

Figure 1. FTIR spectra of (a) pure PPy, (b) PPy-PVA, (c) PPy/Sb_2O_3, and (d) PPy-PVA/Sb_2O_3 nanocomposite

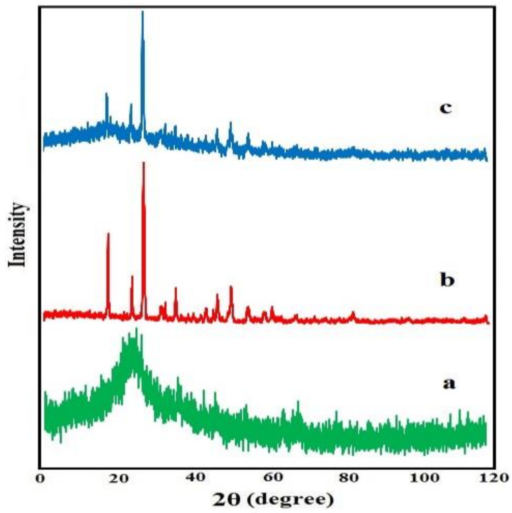

Figure 2. XRD patterns of (a) pure PPy, (b) Sb_2O_3, and (c) PPy/Sb_2O_3 nanocomposite

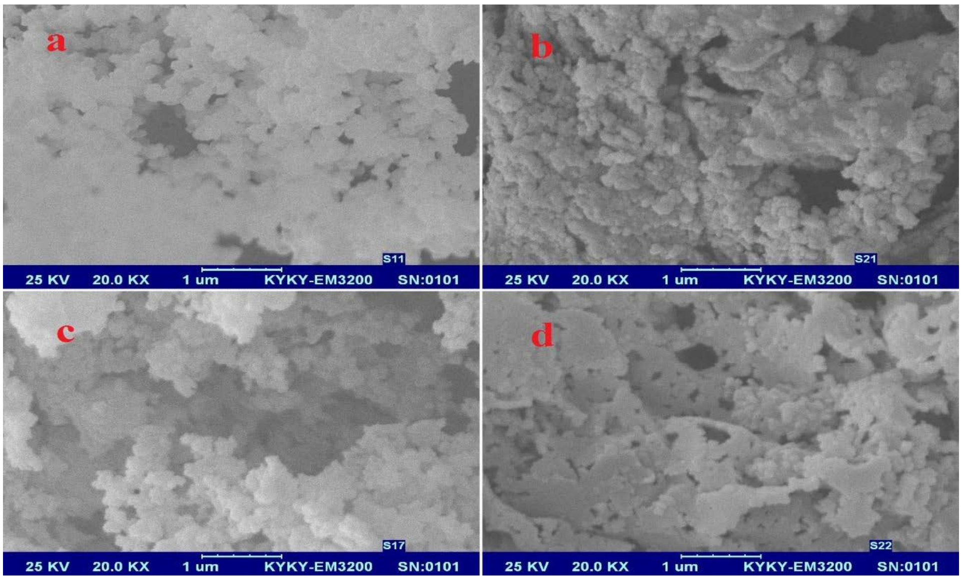

Figure 3. SEM images of (a) pure PPy, (b) PPy-PVA, (C) PPy-Sb_2O_3, and (d) PPy-PVA/Sb_2O_3 nanocomposite

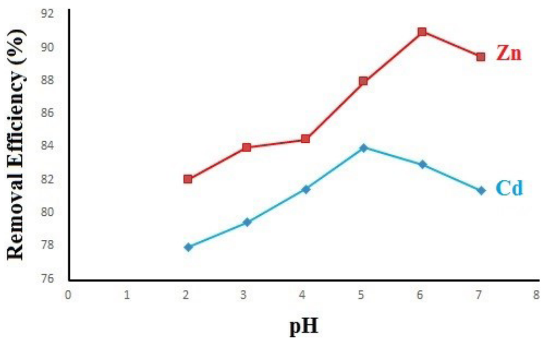

Figure 4. Effect of pH on the removal efficiency with PPy-PVA/Sb_2O_3 (Experimental conditions: Initial concentrations of heavy metal ions for Cd(II) and Zn(II), contact time, and amount of adsorbent were 50 mg/L, 45 min, and 0.3 g, respectively)

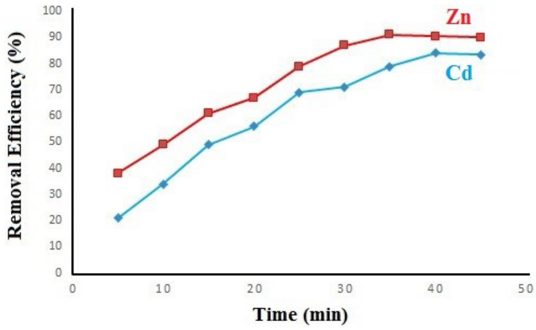

Figure 5. Effect of contact time on the removal efficiency with PPy-PVA/Sb_2O_3 (Experimental conditions: Initial concentrations of heavy metal ions for Cd(II) and Zn(II) and amount of adsorbent were 50 mg/L and 0.3 g, respectively

Effect of contact time

The adsorption efficiency was measured by changing the contact time in the range of 5-45 minutes. The initial concentration of ions was 50 mg/L, and the adsorbent dosage was 0.3 g/30 mL of metal ion solution at the optimized pH (5 for Cd and 6 for Zn) was used. Figure 5 illustrates the uptake of Cd(II) and Zn(II) on PPy-PVA/Sb_2O_3. As seen, adsorption rates for the two metal ions are high at the beginning of the experiment. The initial rapid step may be related to the adsorption of metal ions on open adsorption sites of PPy-PVA/Sb_2O_3. As shown in Figure 5, the removal efficiency of the adsorbent reached the saturation limit after 40 minutes. Therefore, this time can be selected as the equilibration time for subsequent experiments.

Investigation on adsorption isotherm

Adsorption isotherm studies are based on the assumption that each adsorption site is equivalent and independent of the occupation or non-occupancy of adjacent sites. The adsorption isotherm was investigated using concentrations of 25, 50, 75, 100, 150, and 200 mg/L with an adsorbent amount of 0.3 g/30 mL. At constant temperature, the equations describe the relationship between the equilibrium adsorption capacity (q_e) and the equilibrium concentration of metal ions in the solution (C_e), which is essential for modeling adsorption isotherms. To investigate the adsorption capacity of PPy-PVA/Sb_2O_3 for Cd(II) and Zn(II), Langmuir, Freundlich, and Temkin isotherms were used to analyze the experimental data (35). Langmuir (Eq. (3)), Freundlich (Eq. (4)), and Temkin (Eg. (5)) isothermal models could be expressed as given below:

$$Ce/qe = 1/qm\,Kl + Ce/qm \quad (3)$$

$$Log\,qe = Log\,Kf + (1/n)\,LogCe \quad (4)$$

$$qe = at + btLnCe \quad (5)$$

K_L is the Langmuir constant, q_e is the amount of metal adsorbed per specific amount of adsorbent (mg/g), C_e is the equilibrium concentration of the solution (mg/L), q_m is the maximum amount of desired metal ions to produce a monolayer (mg/g), K_F is the Freundlich adsorption isotherm constant (L/g), n is adsorption intensity, b_t is the heat of the adsorption (J/mol), and a_t is the equilibrium binding constant.

The linear plots of adsorption isotherms using PPy-PVA/Sb_2O_3 nanocomposite for the Cd(II) and Zn(II) were shown in Figures 6 and 7, respectively. The Freundlich, Langmuir and Temkin adsorption constants calculated from the isotherms are presented in Table 1. According to R^2 values, it was visible the adsorption for Cd(II) and Zn(II) were well fitted with Langmuir model, indicating the adsorption was a monolayer chemisorption. The maximum theoretical adsorption capacity of PPy-PVA/Sb_2O_3 for Cd(II) and Zn(II) were calculated to be 17.33 and 15.361 mg/g, respectively. The values of n between 1 and 10 ($1/n$ less than 1) indicate a suitable absorption (36).

As shown in Table 1, the values of n for the Freundlich model for both adsorption experiments were obtained greater than 1, indicating a strong interaction between the nanocomposites and Cd(II) and Zn(II). The high R^2 value of the Temkin isotherm also shows that the model matches the data.

Investigation of adsorption kinetics

Adsorption kinetics reveal important information about the rate of adsorption and reaction progress pathways. To investigate the kinetic parameters, the pseudo-first-order kinetic model and the pseudo-second-order model were used. (37). The pseudo-first-order kinetic model can be shown as Eq. (6).

$$Log\left(qe - qt\right) = Log\, qe - \left(K1/2.303\right)t \qquad (6)$$

In this equation, t is the contact time (min), K_1 is the pseudo-first-order rate constant (1/min), q_e and q_t (mg/g) are the equilibrium adsorption capacity and adsorption at time t, respectively. The pseudo-second-order kinetic model can be shown as Eq. (7).

$$t/qt = 1/K2.qe2 + t/qe \qquad (7)$$

K_2 represents the pseudo-second-order rate constant (g/mg.min). The effect of the time parameter on the adsorption of Cd(II) and Zn(II) was investigated by adding 0.3 g of adsorbent to 30 mL of metal ion concentration solution of 50 mg/L with mixing times of 3, 5, 8, 10, 15, 20, 30, 40, 60, 80, 100, 120, 150, and 200 min at room temperature. The

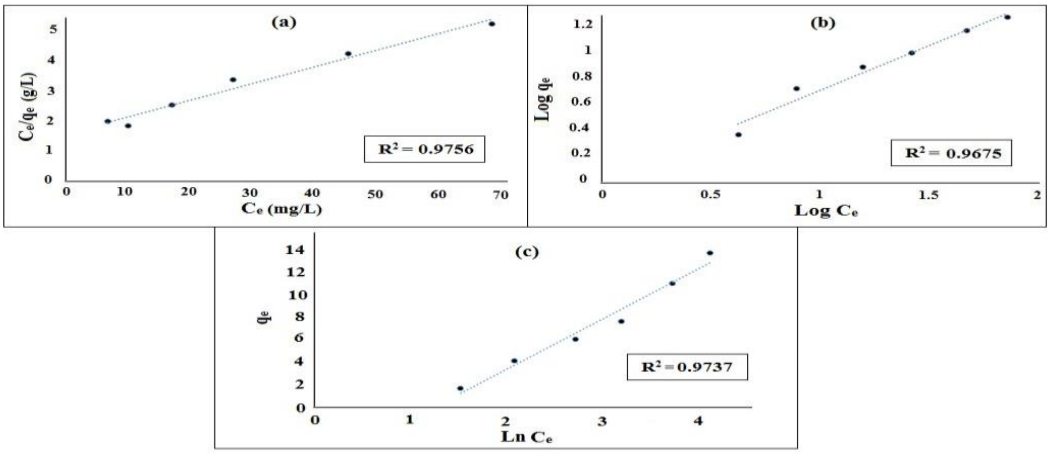

Figure 6. Langmuir (a), Freundlich (b) and Temkin (c) adsorption isotherms linear curve fitting of Cd(II) on PPy-PVA/Sb_2O_3 (Experimental conditions: initial concentrations of heavy metal ion for Cd(II) and amount of adsorbent were 25, 50, 75, 100, 150, 200 mg/L, and 0.3 g, respectively)

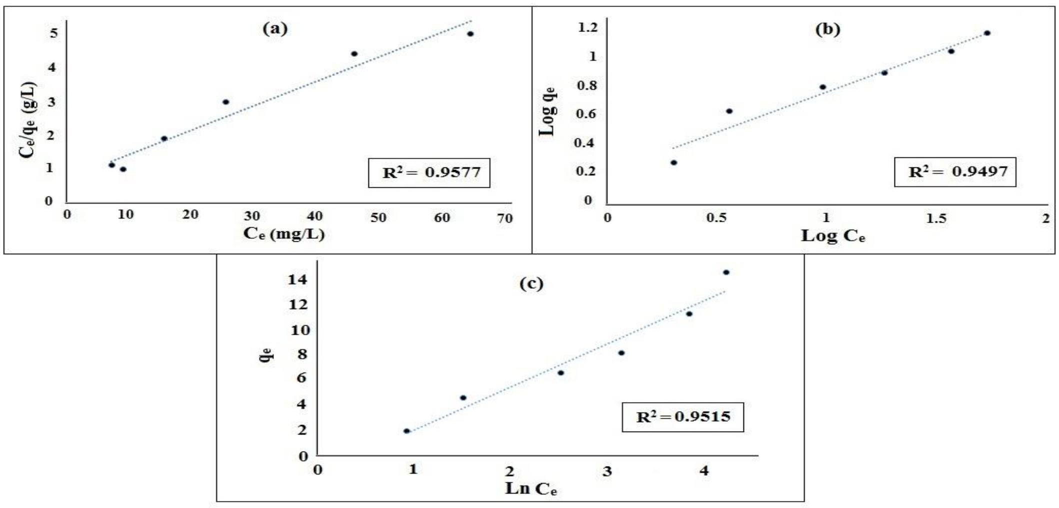

Figure 7. Initial Langmuir (a), Freundlich (b) and Temkin (c) adsorption isotherms linear curve fitting of Zn(II) on PPy-PVA/Sb_2O_3 (Experimental conditions: concentrations of heavy metal ion for Zn(II) and amount of adsorbent were 25, 50, 75, 100, 150, 200 mg/L, and 0.3 g, respectively)

Table 1. Langmuir, Freundlich and Temkin adsorption constants of Cd(II) and Zn(II) adsorption onto the PPy-PVA/Sb_2O_3 nanocomposites

Adsorption isotherm	constants	Cd(II)	Zn(II)
Langmuir	q_m (mg/g)	17.33	15.361
	K_L (L/mg)	0.032	0.061
	R^2	0.9756	0.9577
Freundlich	K_F (L/g)	1.034	1.78
	n	1.68	2.093
	R^2	0.9675	0.9497
Temkin	a_t	-3.4728	-0.6541
	b_t	3.5493	3.0106
	R^2	0.9737	0.9515

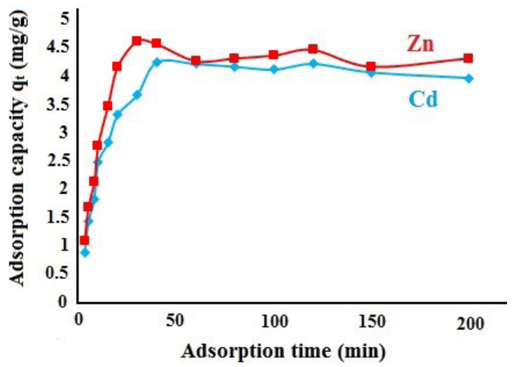

Figure 8. Effect of adsorption time on the adsorption capacity with PPy-PVA/Sb_2O_3

effect of the mixing time factor can be seen in Figure 8. The adsorbed amounts increase sharply and reach the equilibrium after 40 min. K_1, K_2 and q_e are obtained from the slope and the intercept of the corresponding linear plots of $Log\,(q_e\text{-}q_t)$ versus t and t/q_t versus t. The calculation results are shown in Table 2. As could be expected, the correlation coefficients (R^2) of pseudo-second-order kinetics for Cd(II) and Zn(II) in PPy-PVA/Sb_2O_3 were found to be greater than those of the pseudo-first-order kinetic model in all experiments. Also, the q_e^{cal} values calculated by the pseudo-second-order model are very close to the q_e^{exp} values and confirm that the pseudo-second-order model is better in explaining the adsorption conditions.

Thermodynamic study

The solution temperature was changed (25, 35, and 50°C) on a stirrer, in a water bath, and with a thermometer during experiments to investigate the thermodynamic conditions of Cd(II) and Zn(II) ions adsorption on PPy-PVA/Sb_2O_3 nanocomposite. Thermodynamic parameters that include Gibbs free energy change (ΔG), enthalpy change (ΔH), and entropy change (ΔS) are obtained from Eqs. (8) and (9):

$$\Delta G = -RTLnK \quad (8)$$

$$LnK = {}^{S}\!/\!_{R} - {}^{H}\!/\!_{RT} \quad (9)$$

In these equations, T (K) is the absolute temperature, R is the ideal gas constant (8.314 J/mol. K), and K is the thermodynamic equilibrium constant (38). Also, K is equal to the ratio of q_e to c_e as Eq. (10):

Table 2. Kinetic parameters of Cd(II) and Zn(II) adsorption onto the PPy-PVA/Sb_2O_3 nanocomposites

Kinetic models	Parameters	Cd(II)	Zn(II)
Pseudo-first-order	K_1 (1/min)	0.016	0.009
	R^2	0.3254	0.1926
Pseudo-second-order	K_2 (g/mg.min)	0.038	0.051
	q_e (mg/g)	4.238	4.442
	q_e, Experimental	4.237	4.651
	R^2	0.9947	0.9958

$$K = {}^{qe}\!/\!_{Ce} \quad (10)$$

The calculated values for ΔG, ΔH, and ΔS are shown in Table S1. At all temperatures, the negative values of ΔG indicate that the removal of Cd(II) and Zn(II) ions by PPy-PVA/Sb_2O_3 is a spontaneous process that increases with increasing temperature. ΔH values were also positive for all the studied experiments, which confirms the endothermic nature of the adsorption process and shows that the adsorption process is more active with increasing temperature. On the other hand, all the positive values of ΔS indicate that a random increase in the solid-liquid interface occurs during the adsorption of Cd(II) and Zn(II) ions on PPy-PVA/Sb_2O_3. The results obtained from the thermodynamics of the adsorption process, which show that heat increases the adsorption efficiency of metal ions, are consistent with the results of the adsorption isotherm and kinetic studies (38).

Investigating the effect of the concentration of metal ions on adsorption

The concentrations of 25, 50, 80, and 120 (mg/L) of Cd(II) and Zn(II) ions using composites at the optimum experimental conditions were investigated. The amount of adsorbent used was 0.3 g in 30 mL of solution. The results of the effects of Cd(II) and Zn(II) concentration on the removal percentage of nanocomposites are shown in Tables S2 and S3, respectively.

According to the data presented in the tables, the removal percentage increases with the increase in the concentration of metal ions for all composites, and the maximum amount of adsorption of the composites was obtained at a concentration of about 50 mg/L of metal ions. Increasing the number of metal ions in the solution increases the opportunity for the active groups on the adsorbent surface to bind to the metal ion, which leads to an increase in the removal efficiency. Then, with a further increase in the concentration of metal ions in the solution, the adsorption percentage decreased. At higher concentrations, the surfaces and internal cavities of the adsorbents are filled with metal ions, gradually saturated, and as a result, the concentration of metal ions remaining in the solution increases. It should be noted that the removal efficiency of the PPy-PVA composite for both metal ions was better than that of pure PPy, indicating the efficient modification of PPy by PVA. Also, by looking closely at Tables S2 and S3, it can be seen that antimony oxide has a significant effect on the removal percentage. The particle size of the composites decreased with the addition of Sb_2O_3. As a result, the contact surface of the adsorbent increases, which subsequently improves the removal percentage.

For a deeper understanding, Brunauer-Emmett-Teller (BET) measurements were performed on the surface of the composites. PPy-PVA/Sb_2O_3 nanocomposite showed the highest surface area with 27.61 m^2/g compared to pure PPy and PPy/Sb_2O_3 composite, which were 6.27 and 15.63 m^2/g, respectively. As seen in the SEM image of PPy-PVA/Sb_2O_3, the increase in surface area is consistent with the decrease in particle size. Therefore, it can be concluded that increasing the surface area of PPy-PVA/Sb_2O_3 increases the removal percentage.

Discussion

Adsorption mechanism

Two different mechanisms can be considered in the adsorption of heavy metal ions on PPy-PVA/Sb_2O_3: (I) physical adsorption on the surface of PPy-PVA/Sb_2O_3 and (II) Chemisorption due to the reaction between PPy molecules with Cd(II) and Zn(II) ions. The synthesized composites based on polypyrrole have a spherical and porous structure with a high specific surface area. Therefore, metal ions can penetrate the adsorbent structure due to the porosity and holes and be adsorbed on the surfaces and gaps of the composites. Another adsorption mechanism that most likely occurs on the PPy/Sb_2O_3 surface is through the electrostatic interaction of hydroxyl or chelation groups with N atoms located in the PPy structure and metal ions. It can be stated that the interaction between ions and the PPy matrix is the result of hybridization between the non-bonded pair of nitrogen atoms in the structure of polypyrrole and the empty orbital of metal ions such as Cd(II) (39,40). On the other hand, nitrogen species of PPy play a significant role in the process of reducing the polymer-metal interface.

Study of Desorption and Reusability

The recovery and reuse of an adsorbent is an important issue because it is related to the Current operating cost of the adsorption process. Desorption experiments were performed to regenerate the Cd(II) and Zn(II) loaded PPy-PVA/Sb_2O_3 composite for adsorbent reuse. First, for the adsorption of Cd(II) and Zn(II), 0.1 g PPy-PVA/Sb_2O_3 was contacted with 50 mL of 100 ppm Cd(II) and Zn(II) solution at pH 5 and 6, respectively. Desorption of Cd(II) and Zn(II) loaded PPy-PVA/Sb_2O_3 adsorbent was done using 50 mL of 1 M NaOH solution. NaOH solution was used because it can reduce the electrostatic attraction force and also reduce the stability in the polypyrrole chain. The regenerated PPy-PVA/Sb_2O_3 was investigated for six consecutive adsorption-desorption cycles to confirm the reusability of the adsorbent (Figure S1). The percentage of adsorption of the recycled adsorbent was 98.66% and 97.24% at the first cycle for Cd(II) and Zn(II), respectively. From the fifth cycle, the removal efficiency starts to decrease with a low gradient. This is due to incomplete desorption of metal ions. The test results show that the PPy-PVA/Sb_2O_3 composite can be successfully reused for four consecutive adsorption-desorption cycles with the least possible decrease in its removal efficiency. Hence, the PPy-PVA/Sb_2O_3 nanocomposite can be used as a high-performance and recyclable adsorbent for the adsorption of heavy metal ions.

Conclusion

In this study, the nanocomposites of polypyrrole (PPy/Sb_2O_3) were synthesized in the presence of poly(vinyl alcohol) (PVA) to adsorb Cd(II) and Zn(II) ions from water. The synthesized composites were analyzed by Fourier transform-infrared (FTIR) spectroscopy, X-ray diffraction (XRD), and scanning electron microscopy (SEM). The results indicated that the Sb_2O_3 and PVA influenced the properties of synthesized nanocomposites. Adsorption experiments were carried out in a batch to remove heavy metal ions from aqueous solutions. The parameters affecting the adsorption process, including pH, contact time, and initial metal ion concentration, were investigated. The adsorption isotherms for Cd(II) and Zn(II) on PPy-PVA/Sb_2O_3 were well fitted with the Langmuir model. The maximum theoretical adsorption capacities for Cd(II) and Zn(II) were calculated to be 17.33 and 15.361 mg/g, respectively. The kinetic results indicate that the pseudo-second-order kinetic model provides a better description of the adsorption process. Moreover, the thermodynamic parameters show the endothermic and spontaneous nature of the current adsorption process with an increase in PPy-PVA/Sb_2O_3. Based on these results, polypyrrole and its nanocomposites have potential for use as effective adsorbents due to their ease of synthesis, low cost, and regeneration efficiency for the removal of heavy metal ions from aqueous solutions.

Acknowledgments

The authors sincerely thank the Department of Chemical Engineering of Mazandaran University for creating a suitable environment for conducting the research, as well as the support and guidance provided during this study.

Authors' Contribution

Conceptualization: Zeynab Karimi, Ali Akbar Amooey, Reza Khalili.
Data Curation: Ali Akbar Amooey Zeynab Karimi.
Formal Analysis: Reza Khalili, Zeynab Karimi, Amirhossein Alidadi.
Investigation: Reza Khalili, Soheil Balsini Gavanaroudi, Amirhossein Alidadi.
Methodology: Reza Khalili, Ali Akbar Amooey, Saeid Sabzehali, Amirhossein Alidadi.
Project Administration: Zeynab Karimi, Reza Khalili.
Resources: Reza Khalili, Zeynab Karimi.
Software: Reza Khalili, Soheil Balsini Gavanaroudi.
Supervision: Reza Khalili, Zeynab Karimi.
Validation: Zeynab Karimi, Ali Akbar Amooey, Reza Khalili.
Visualization: Ali Akbar Amooey Saeid Sabzehali.
Writing – Original Draft: Ali Akbar Amooey, Reza Khalili.
Writing – Review & Editing: Ali Akbar Amooey, Reza Khalili.

Competing Interests
The authors declare that they have no known competing financial interests or personal relationships that could have appeared to influence the work reported in this paper.

Ethical Approval
This study was conducted in compliance with ethical principles and guidelines, guaranteeing the right to human protection, safe handling of dangerous substances, and scientific integrity. Authors adhere to ethical standards in their research and reports to contribute to the advancement of knowledge.

Funding
This research did not receive any financial support from any public or commercial funding organization.

Supplementary Files
Supplementary file 1 contains Tables S1-S3 and Figure S1.

References

1. Kgabi DP, Ambushe AA. Removal of Pb(II) ions from aqueous solutions using natural and HDTMA-modified bentonite and kaolin clays. Heliyon 2024;10(18) :e38136. doi:10.1016/j.heliyon.2024.e38136
2. Zhao S, Li Q, Tang Z, Yang Y, Wu J, Gao P, et al. Simultaneous removal of Cr, Cu, Zn, and Cd by nano zero-valent iron modified sludge biochar in high salinity wastewater. Sep Purif Technol 2024;347:127560. doi:10.1016/j.seppur.2024.127560
3. Fu H, Sheng J, Tang C, Zhang WX, Ling L. Simultaneous removal of Cd(II) and phosphate by nanoscale zero-valent iron from solution: co-sorption and implication of corrosion. Chemosphere 2024;364:143160. doi:10.1016/j.chemosphere.2024.143160
4. Ye Z, Jiang M, Yan F, Cao B, Wang F. Chemical aging of biochar-zero-valent iron composites in groundwater: impact on Cd(II) and Cr(VI) co-removal. Environ Res 2024;263(Pt 1):120022. doi:10.1016/j.envres.2024.120022
5. Ryabchenko EO, Suslov AP, Morozov NA, Krivoshapkina EF. Silica/carbon dot nanosorbent for the detection and removal of Pb(II) and Co(II) ions from wastewater. Chem Eng J 2024;500:156610. doi:10.1016/j.cej.2024.156610
6. Ahmer MF, Uddin MK. Structure properties and industrial applications of anion exchange resins for the removal of electroactive nitrate ions from contaminated water. RSC Adv 2024;14(45):33629-48. doi:10.1039/d4ra03871a
7. Mohamed Noor MH, Ngadi N. Global research landscape on coagulation-flocculation for wastewater treatment: a 2000-2023 bibliometric analysis. J Water Process Eng 2024;64:105696. doi:10.1016/j.jwpe.2024.105696
8. Rajyaguru A, Seigneur N, Bildstein O, Savoye S, Wittebroodt C, Hôpital EL, et al. Barite and gypsum precipitation in chalk: a numerical simulation approach revealing the coupled impact of physical and chemical heterogeneities in porous media. Chem Geol 2022;609:121069. doi:10.1016/j.chemgeo.2022.121069
9. El-Sabban HA, Mubarak MF, Diab MA. PPy-NTs/C/TiO2/poly(ether sulfone) porous composite membrane: efficient ultrafiltration of Evans blue dye from industrial wastewater. Synth Met 2023;297:117383. doi:10.1016/j.synthmet.2023.117383
10. Garcia-Rodriguez O, Fang C, Jiang H, Deng J, Imbrogno J, Swenson TM, et al. Electrochemical oxidation of a membrane-distillation concentrate for the treatment of real pharmaceutical wastewater. Chemosphere 2024;367:143527. doi:10.1016/j.chemosphere.2024.143527
11. Mostafaeipour A, Qolipour M, Rezaei M, Babaee-Tirkolaee E. Investigation of off-grid photovoltaic systems for a reverse osmosis desalination system: a case study. Desalination 2019;454:91-103. doi:10.1016/j.desal.2018.03.007
12. Park S, Kim I, Han I, Oh H. Advanced electro-oxidation-adsorption process for chlorate removal from synthetic and municipal wastewater treatment effluents. Desalin Water Treat 2024;320:100877. doi:10.1016/j.dwt.2024.100877
13. Liu C, Wang W, Wang N, Liu Z, Shen P, Hu J, et al. Synthesis of cubic mesoporous silica SBA16 functionalized with carboxylic acid in a one-pot process for efficient removal of wastewater containing Cu2+: adsorption isotherms, kinetics, and thermodynamics. Microporous Mesoporous Mater 2025;382:113402. doi:10.1016/j.micromeso.2024.113402
14. Geng M, Zeng T, Deng X, Zhang Z, Xiao C, Chi Ra. Innovative strategies for ammonia nitrogen removal in rare earth tailings: an advanced element recycling process using leaching, chemical precipitation and adsorption. J Water Process Eng 2024;67:106205. doi:10.1016/j.jwpe.2024.106205
15. Lee JI, Jeong Y, Lee YJ, Lee CG, Park SJ. Harnessing wood bottom ash for efficient arsenic removal from wastewater: adsorption mechanisms and process optimisation. Chemosphere 2024;364:143204. doi:10.1016/j.chemosphere.2024.143204
16. Bhaskar S, Rashmi Shree KN, Apoorva KV, Sreenivasa MY. Adsorption - advanced oxidation process (AAOP) for the heavy metals and organic matter removal from leachate using combined filtration-Fenton's and photo-Fenton's treatment. J Environ Manage 2024;371:123009. doi:10.1016/j.jenvman.2024.123009
17. Tan B, Gou G, Ren Y, Fang Z, Liu C, Lai B, et al. Comparative study of organic removal by pre-adsorption oxidation and synchronous adsorption oxidation processes: performance and mechanism. J Hazard Mater 2024;474:134784. doi:10.1016/j.jhazmat.2024.134784
18. Asayesh-Ardakani E, Rahmani M, Hosseinian A, Ghaffari SB, Sarrafzadeh MH. Improvement strategies on application of covalent organic frameworks in adsorption, photocatalytic, and membrane processes for organic pollution removal from water. Coord Chem Rev 2024;518:216087. doi:10.1016/j.ccr.2024.216087
19. Wang J, Li X, Lan Y, Wang H, Ma X, Wang H, et al. Study on the adsorption mechanism of ciprofloxacin in wastewater by modified fly ash under the coexistence of copper. J Environ Chem Eng 2024;12(6):114336. doi:10.1016/j.jece.2024.114336
20. Nguyen CH, Juang RS. Efficient removal of methylene blue dye by a hybrid adsorption-photocatalysis process using reduced graphene oxide/titanate nanotube composites for water reuse. J Ind Eng Chem 2019;76:296-309. doi:10.1016/j.jiec.2019.03.054
21. Sheraz N, Shah A, Haleem A, Iftikhar FJ. Comprehensive assessment of carbon-, biomaterial- and inorganic-based adsorbents for the removal of the most hazardous heavy metal ions from wastewater. RSC Adv 2024;14(16):11284-310. doi:10.1039/d4ra00976b
22. Kouotou D, Gharibi EK, Bailón-García E, Ghalit M. Improved Cd(II) ions removal performance from aqueous solution using cerium doped activated carbon. Mater Today Proc 2022;51:1957-65. doi:10.1016/j.matpr.2021.04.298
23. Wang C, Yu J, Feng K, Wang L, Huang J. Synthesis of porous magnetic zeolite-based material and its performance on removal of Cd2+ ion and methylene blue from aqueous solution. Microporous Mesoporous Mater 2022;345:112256. doi:10.1016/j.micromeso.2022.112256
24. Saberian MK, Kargari A, Soleimani M, Alaei Shahmirzadi MA, Mofarrah E. Kinetics and equilibrium study of adsorptive removal of cadmium ions from aqueous solutions by utilizing lime peel as a biosorbent. Desalin Water Treat 2023;297:88-101. doi:10.5004/dwt.2023.29590
25. Zhang F, He S, Xi L, Ma L, Zhang L, Xiong L, et al. Polypyrrole/waste molasses composites as a superior adsorbent for highly efficient and selective removal of Cr(VI) from aqueous environments. Surf Interfaces 2024;51:104726. doi:10.1016/j.surfin.2024.104726
26. Huang F, Tian X, Wei W, Xu X, Li J, Guo Y, et al. Wheat straw-core hydrogel spheres with polypyrrole nanotubes for

the removal of organic dyes. J Clean Prod 2022;344:131100. doi:10.1016/j.jclepro.2022.131100
27. Senguttuvan S, Janaki V, Senthilkumar P, Kamala-Kannan S. Polypyrrole/zeolite composite - a nanoadsorbent for reactive dyes removal from synthetic solution. Chemosphere 2022;287(Pt 2):132164. doi:10.1016/j.chemosphere.2021.132164
28. Cao F, Sun Y, Zhang L, Sun J. High efficient adsorption accompanied by in-situ reduction of Cr(VI) removal by rice straw fiber ball coated with polypyrrole. Appl Surf Sci 2022;575:151583. doi:10.1016/j.apsusc.2021.151583
29. Abdel Rehim MH, Badawy AA, Turky G. Electrical properties and heavy ions removal ability of graphitic carbon nitride/ polypyrrole composite. J Phys Chem Solids 2022;167:110741. doi:10.1016/j.jpcs.2022.110741
30. Girija S, Karthika S, Wilson J. ZIF-12@polypyrrole nanowires for selective detection of cadmium ions in water samples. Results Chem 2024;7:101527. doi:10.1016/j.rechem.2024.101527
31. Ballav N, Maity A, Mishra SB. High efficient removal of chromium(VI) using glycine doped polypyrrole adsorbent from aqueous solution. Chem Eng J 2012;198-199:536-46. doi:10.1016/j.cej.2012.05.110
32. Marandi M, Kallip S, Matisen L, Tamm J, Sammelselg V. Formation of nanometric polypyrrole films on Au(111): a STM, SEM and XPS study. Synth Met 2012;162(1):162-70. doi:10.1016/j.synthmet.2011.11.026
33. Chavan UD, Prajith P, Kandasubramanian B. Polypyrrole based cathode material for battery application. Chem Eng J Adv 2022;12:100416. doi:10.1016/j.ceja.2022.100416
34. Zhao Y, Zhao C, Yang Y, Li Z, Qiu X, Gao J, et al. Adsorption of sulfamethoxazole on polypyrrole decorated volcanics over a wide pH range: mechanisms and site energy distribution consideration. Sep Purif Technol 2022;283:120165. doi:10.1016/j.seppur.2021.120165
35. Peng H, Shen Y, Luo M, Zheng X, Wen J. Polypyrrole-decorated Mg-Al layered double oxides for dye adsorption: isotherm, kinetics, and thermodynamic investigations. Chem Phys Lett 2023;824:140568. doi:10.1016/j.cplett.2023.140568
36. Choe J, Ji J, Yu J, Jang K, Yun J, Choe S, et al. Adsorption of Cr(VI) in aqueous solution by polypyrrole nanotube and polypyrrole nanoparticle; kinetics, isotherm equilibrium, and thermodynamics. Inorg Chem Commun 2022;145:109981. doi:10.1016/j.inoche.2022.109981
37. Olad A, Ahmadi S, Rashidzadeh A. Removal of nickel(II) from aqueous solutions with polypyrrole modified clinoptilolite: kinetic and isotherm studies. Desalin Water Treat 2013;51(37-39):7172-80. doi:10.1080/19443994.2013.771285
38. Seyedi Marghaki N, Abkari Jonoush Z, Rezaee A. Chromium(VI) removal using microbial cellulose/ nano-Fe3O4@polypyrrole: isotherm, kinetic and thermodynamic studies. Mater Chem Phys 2022;278:125696. doi:10.1016/j.matchemphys.2022.125696
39. Sarojini G, Venkateshbabu S, Rajasimman M. Facile synthesis and characterization of polypyrrole - iron oxide - seaweed (PPy-Fe(3)O(4)-SW) nanocomposite and its exploration for adsorptive removal of Pb(II) from heavy metal bearing water. Chemosphere 2021;278:130400. doi:10.1016/j.chemosphere.2021.130400
40. Mansoor SJ, Abbasitabar F. Adsorption behavior of Fe(II) and Fe(III) ions on polyaniline coated sawdust: batch and fixed-bed studies. Acta Chim Slov 2020;67(1):36-46. doi :https://doi.org/10.17344/acsi.2019.5121